Jefferson Lab
E01-015 Technical Note 1
August 31, 2005

Detection Efficiency of the Neutron Detector

Ramesh Subedi[1], Douglas Higinbotham[2], John Watson[1],
Olivier Gayou[3], Shalev Gilad[3], Peter Monaghan[3], Eli Piasetzky[4], Ran Shneor[4], Steve Wood[2].

[1] Kent State University, Kent, OH 44242.

[2] Thomas Jefferson National Accelarator Facility, Newport News, VA 23606.

[3] Massachusetts Institute of Technology, Cambridge, MA 02139.

[4] Tel Aviv University, Tel Aviv 69978, Israel.

Abstract

We discuss how the neutron detection efficiency of the neutron detector for the experiment E01-015 is determined using a computer simulation code. We also describe how we find neutron transmittance of various materials through which the neutron beam passes. The product of the efficiency and the transmittance determines how many neutrons are detected out of the total neutrons incident on the neutron detector. This number turns out to be about 17% for the neutrons of kinetic energy above about 60 MeV.

Contents

1. Neutron Detector

The experiment E01-015 uses a large volume neutron detector having 88 plastic scintillator bars split into four planes. Each bar is 10 cm thick in the beam direction while the bar heights [1] along transverse to the beam direciton is different in different planes. The height is 10 cm for any bars in the first plane, 12.5 cm for the second plane and 25 cm in the fourth plane. The third plane contains bars of mixed heights namely 10 cm, 12.5 cm and 15 cm as explained by the color code in Fig.1 below. Bars of same height have same color in any planes in this figure. In addition, the detector also has a veto layer made up of two centimeter thick 64 plastic bars residing in front of the first plane. Thirty two rows of two end-to-end overlaping veto paddles form the veto plane (not shown in Fig.1.).

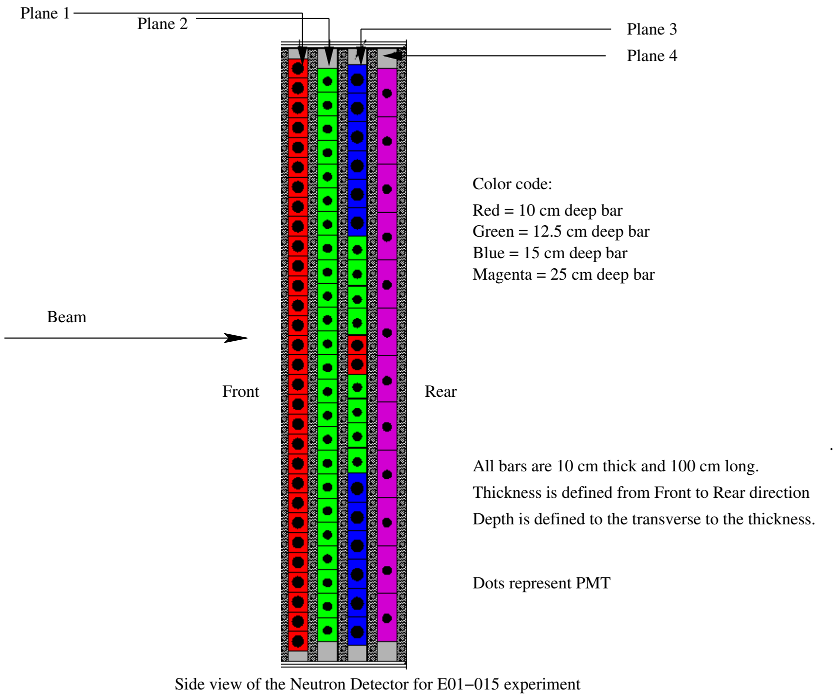

Fig. 1 Neutron Detector for the experiment E01-015

2. Neutron Threshold

The neutron detection efficiency of a neutron detector strongly depends upon a threshold value set for a neutron to be detected. At higher threshold the neutron detection efficiency is lower and vice-versa. We use the following plot (Fig.2) to define software thresholds of bars in various planes of the neutron detector. According to fig 2, out of the four vertical planes in the neutron detector,

[1] height is depth in Fig. 1 .

plane one has threshold of 5.3 MeVee while plane two has 4.4 MeVee, plane three has 4.7 MeVee and plane four has 7.1 MeVee. For some reason which is not clear yet, we needed to increase the software threshold seen in fig 2 by extra eighty percent in order to match the detection efficiency calculated from the simulated data to that found from the experimental data. Note that the term "detection efficiency" coined here is the product of transmittance and efficiency which will be described in subsequent sections.

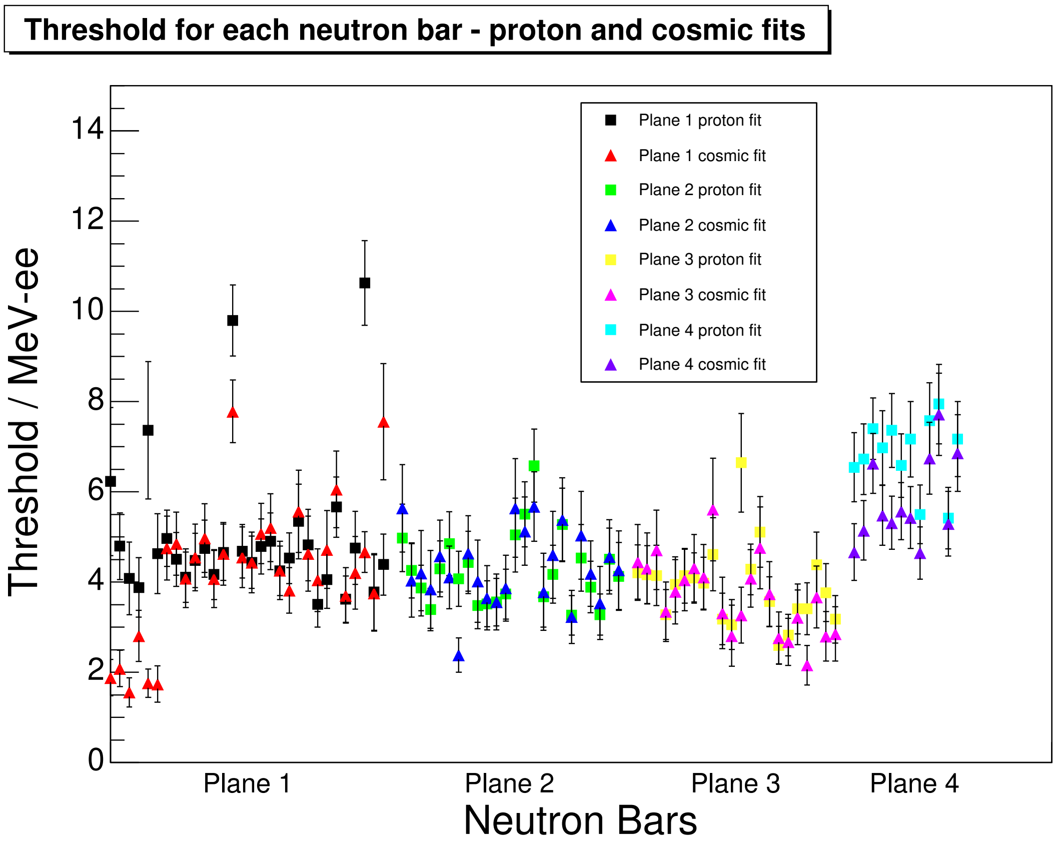

Fig. 2 Threshold plot of the Neutron Detector bars.

We had set different thresholds in the neutron detector discriminators for different run periods. All 4-pass (4.6 Gev beam) data had neutron detector discriminator threshold (a hardware threshold) as -50 mV. The software threshold in MeVee mentioned above belong to this part of the experimental data. All 2-pass (2.345 GeV beam) data on liquid deuterium runs belong to -100 mV hardware threshold and we find the software threshold for this part of the data as the double in value for that of 4-pass beam data.

3. Efficiency

We use the computer simulation code developed by R.Cecil et al [1] to determine the efficiency (ϵ) of neutron detection of a scintillator paddle. The input file to the code for this work is shown in Appendix A. Shown in Fig.3 below is a typical efficiency plot obtained from the simulation code. The data table for the plots is given in Table 1 in Appendix B. What is plotted here is the efficiency of a neutron counter versus kinetic energy of neutrons. The efficiency determines how many neutrons are detected out of the total incident neutrons on the neutron counter. Note that the code does not care about the history of the neutron flight before it hits the counter. This means that in order to know the history, for example, what fraction of the neutrons were removed from the beam due to an absorbing materials present before the neutron counters, we need to know the neutron transmittance of the absorber which is desribed in section 4 below. The peak between 40 to 60 MeV in the trace (fig 3) of each plane indicates the onset of scattering from carbon. Below the peak the n-p elastic scattering dominates while after the peak all reaction channels open up and saturate the efficiency.

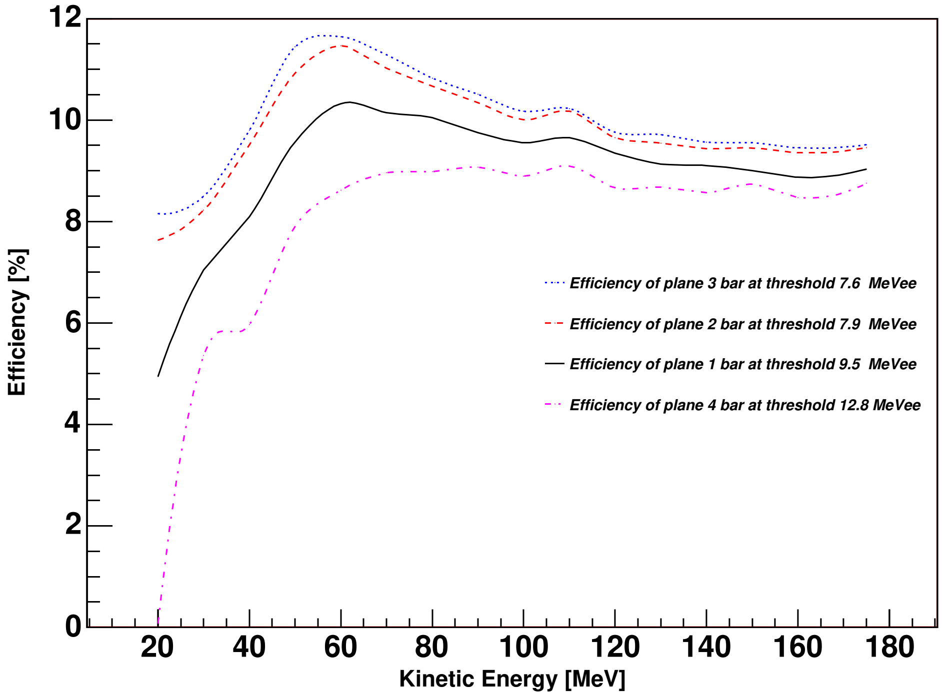

Fig. 3 Efficiency versus kinetic energy plots for neutron counters.

4. Transmittance

To determine how many neutrons are really incident on the neutron detector depends upon what fraction of neutrons are attenuated in the material present between the target and the neutron detector. In order to see this fraction we need transmittance.

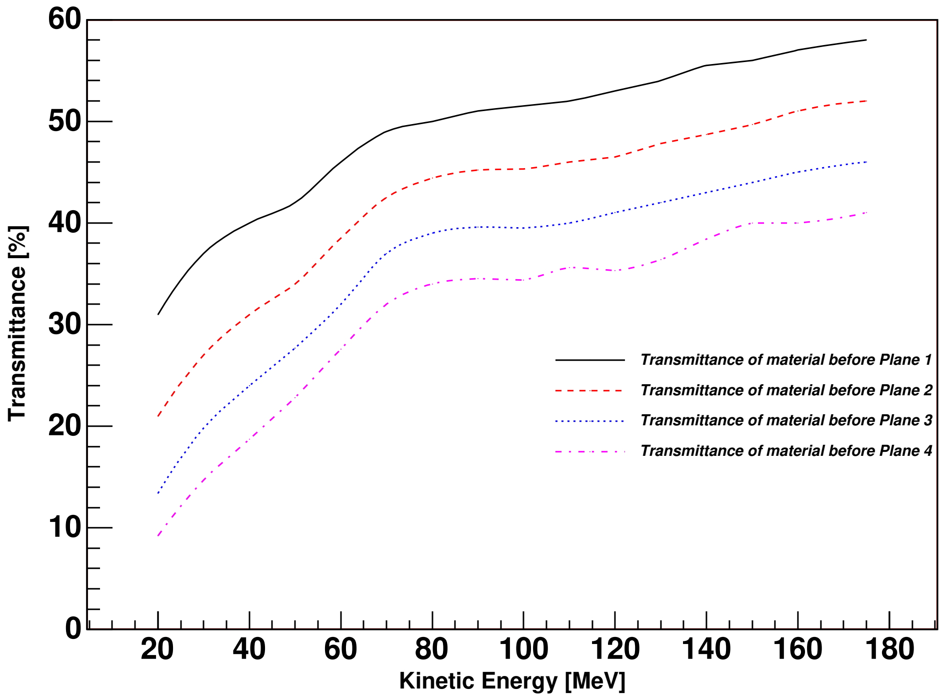

Fig. 4 Transmittance versus kinetic energy plots for different material combinations

The transmittance (T) of a neutron is given by an expression:

$$T = e^{-\sigma n L}$$

where
σn = attenuateion
σ = removal cross section of a neutron
n = number density of a material = N.ρ /A
N = Avogadro number
ρ = density of the material

A = Atomic weight of the material
L = thickness of the material.

The Fig.4 above shows the transmittance of a combination of materials such as air, iron, lead and plastic of various thicknesses before the plane under consideration. Data for this figure are given in Table 4 in Appendix D.

The "Removal cross section" represents the probability that a neutron will be removed from the beam. The removed neutron will not be detected by the neutron detector. Removal cross section can not be obtained directly from a cross section table since its definition depends upon how one defines for his specific purpose due to the location of the detector from the target and the medium beteween them which may remove neutrons from the beam. If such medium is close to the target and hence far from the detector then the total cross section can also contribute to the removal cross section. In our case lead wall is close to the neutron detector. The space between the back face of lead wall and the front face of neutron detector is 56 cm and the neutron detedector sits 6 meter from the target. Thus the total cross section of neutrons in lead wall does not contribute to the removal cross section.

Total cross section is given as the sum of elastic cross section and non elastic cross section. Elastic cross section is strongly peaked near zero degree about the beam direction. We define removal cross section as a "non elastic" cross seciton which includes everything but the elastic cross section. Note that the non elastic cross section is not an inelastic cross section. For a given substance the non elastic cross section necessarily has an upper limit equal to the total cross section and a lower limit equal to the inelastic cross section. Non elastic cross section can be obtained from the cross section table [2] . For hydrogen, non elastic cross section is not available in the cross section table. We define removal cross section for hydrogen as the two third of the total cross section. We need hydrogen cross section to determine transmittance of a scintillator plastic which is made up of hydrogen and carbon in the H to C ratio 1.104. All used cross section data are shown in Appendix C.

We have 600 cm of air, 4 cm of veto counters, 3.55 cm of BigBite plastic scintillators and 9.08 cm of lead wall (made up of 4 cm thick iron and 5.08 cm thick lead) between the target and the neutron detector. We assume that the total cross section of non of these materials does contribute to the removal cross section. We get low cross section of neutrons when they interact feebly in the material while we get high cross section of neutrons when they interact highly in the material. At lower cross section the transmittance is higher and vice-versa. To calculate the total transmittance of neutrons through these materials we use the following relation.

$$T_{total} = [e^{-\sigma n L}]_{air} \ * \ [e^{-\sigma n L}]_{plastic} \ * \ [e^{-\sigma n L}]_{Fe} \ * \ [e^{-\sigma n L}]_{Pb}$$

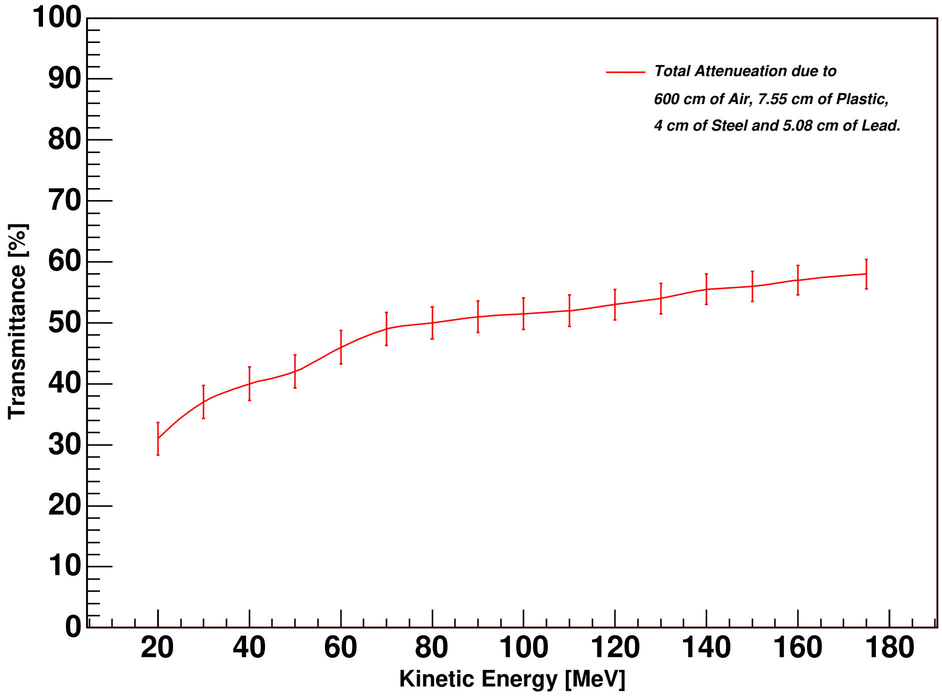

Fig. 5 Transmittance versus kinetic energy plot

Defining an error in σ as [2]

$$\triangle\sigma = \pm\ \sigma/4,$$

we find, assuming no error in nL, the error in T_{total} as

$$\triangle T_{total} = \pm\ T_{total}\ *\ [\ \sqrt{[\sigma nL]^2_{air} + [\sigma nL]^2_{plastic} + [\sigma nL]^2_{Fe} + [\sigma nL]^2_{Pb}}\ \ ]/4$$

Shown above in Fig.5 is a typical plot showing the total trnansmittance of various materials that was placed in front of plane one. Data for the Fig. 5 are shown in Table 5 in Appendix D. The error in the transmittance is close to $\pm$ 5% due to an error of $\pm$25% [3] in removal cross section.

[2]For an expression x = a + b + c + ..., the error in x is $\triangle x = \sqrt{[\triangle a]^2 + [\triangle b]^2 + [\triangle c]^2 + ...}$, while for an expression x = e^a, the error in x is $\triangle x = x * \triangle a$.

5. Detection Efficiency

5.1 First Method

We define the product of Transmittance (T) and efficiency ϵ as the neutron detection efficiency and simply call detection efficiency henceforth. Shown below in Fig. 6 in green line is the detection efficiency of the neutron detector as a function of neutron kinetic energy. Other differently colored histograms are the same quantity for different planes as explained in the figure. Data for this figure are shown in Table 6 in Appendix D.

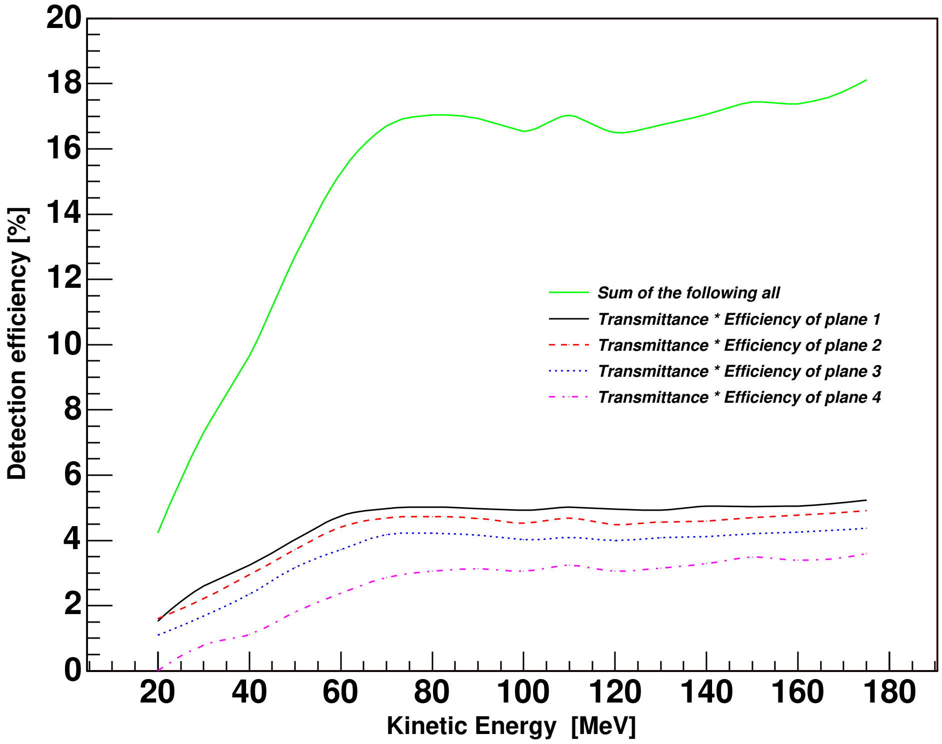

Fig. 6 Detection efficiency versus kinetic energy plots for the Neutron Detector

The procedure of detection efficiency calculation in fig 6 is the following:

• Plane 1: Product of efficiency of one paddle in plane 1 and the transmittance of air, lead wall and plastic of 7.55 cm (plastic from BigBite bars + veto paddle). Veto thickness is taken as 4 cm for this purpose due to the overlap of two veto paddles at the middle.

• Plane 2: Product of efficiency of one paddle in plane 2 and the transmittance of air, lead wall and plastic of 17.55 cm (plastic from BigBite bars + veto paddle + a bar in plane 1).
• Plane 3: Product of efficiency of one paddle in plane 3 and the transmittance of air, lead wall and plastic of 27.55 cm (plastic from BigBite bars + veto paddle + a bar in plane 1+ a bar in plane 2).
• Plane 4: Product of efficiency of one paddle in plane 4 and the transmittance of air, lead wall and plastic of 37.55 cm (plastic from BigBite bars + veto paddle + a bar in plane 1+ a bar in plane 2 + a bar in plane 3).

The detection efficiency is the sum of the product of the efficiency and the transmittance of all the four planes.

5.2 Second Method

We have also calculated the same detection efficiency as shown in fig 6 using a different approach which is shown in fig 7 below. The data for this figure are shown in Table 7 in Appendix D.

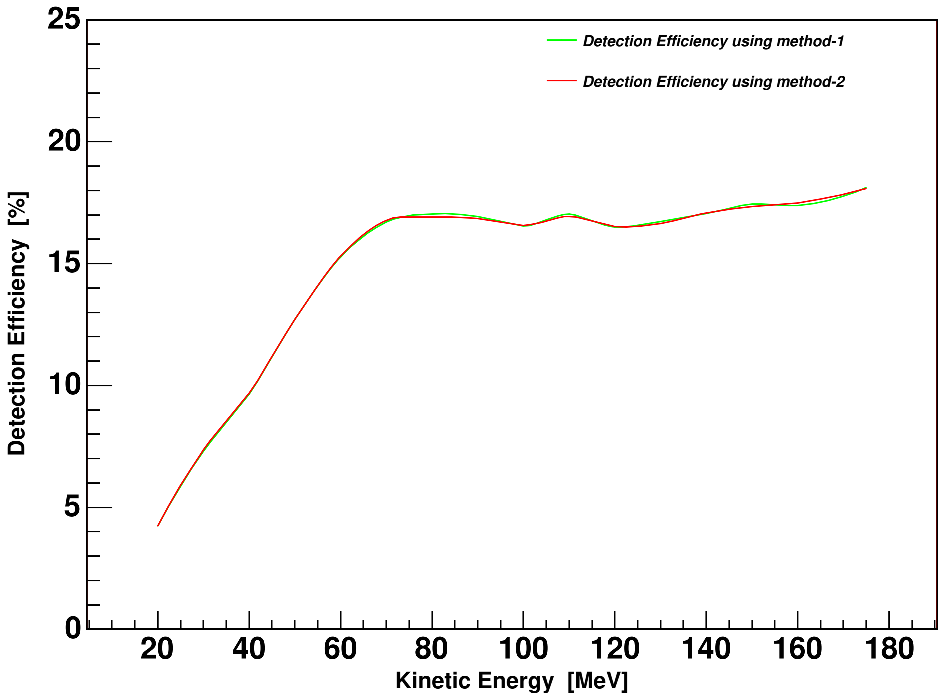

Fig. 7 Detection efficiency versus kinetic energy using the first method(green) and using the second method (red). Both traces overlap perfectly.

The procedure of calculating detection efficiency in Fig. 7 is the following:
•Step 1: Find transmittance of all scintillator plastic which is in front of plane 1.
•Step 2: Find transmittance of all scintillator plastic which is in front of the plane under consideration.
•Step 3: Find a factor dividing the result of Step 2 by that of Step 1. This factor determines what fraction of neutron flux is incident on the plane under consideration taking the flux incident on the first plane as 100%. A table of this factor is shown in Table 3A in Appendix D.

Here is a physical relation involved that agrees with the findings of the above processes:

$$F_n = (f)^{n-1}$$

where
f = factor for plane 2,
F_n = factor for n^{th} plane and n $\geq$3.
•Step 4: Find efficiency from the computer simulation code for a bar in a plane under consideration.
•Step 5: Multiply the results of Step 3 and Step 4.
•Step 6: Multiply the result of step 5 by the transmittance of all materials before plane 1.
•Step 7: Repeat Step 6 for all four planes. Sum the result for each kinetic energy point.

This result is shown as red line in Fig. 7. The values of the detection efficiency calculated using both approaches agree quite well since the both traces in fig 7 overlap perfectly.

6. Experimental and Simulated Data Together

Fig 8 shows the experimental data plotted on top of the simulated data. The dot-dashed and solid curves are produced from simulated data while the data points about these curves are from the experiment. The simulated blue trace is from the runs of 2-pass (2.345 GeV) beam on liquid deuterium while the magenta trace is from the runs of 4-pass (4.6 GeV) beam on liquid deuterium. First two and the last three blue data points are little bit off from the predicted values. The reason for this to the first two data points could not be due to the neutron counter's edge effect since they are higher in position than the prediected values but could be due to the extra eighty percent increase of software threshold in such a low efficiency region. The last three blue points are far from the predicted values simply due to the bar's edge effect. Since we did not have many runs at 4.6 GeV beam on liquid deuterium, we could not get many data points for the magenta data points and also the error bars are high there.

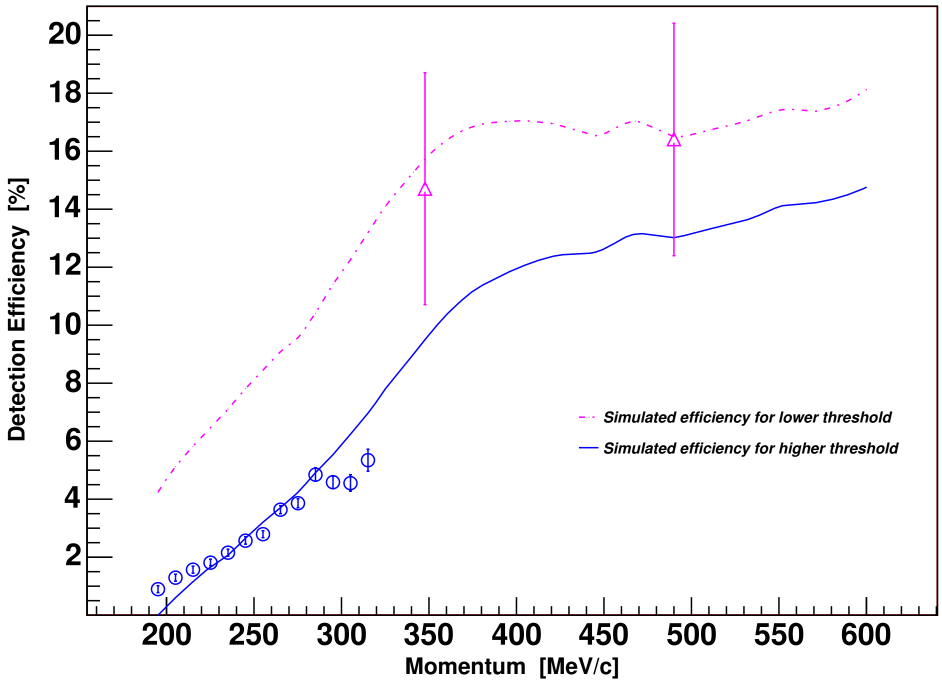

Fig. 8 Detection efficiency versus momentum plots. Data points are from the experiment while the dot-dashed and smooth traces are from simulation. Magenta dot-dashed trace for 4-pass (4.6 GeV) beam and blue solid trace for 2-pass (2.345 GeV) beam.

7. Conclusion

With the incrrease of neutron kinetic energy, the efficiency of any counter first increases and then slowly decreases while the transmittance always increases so that the product of these two quantities remains almost constant. This product, called as detection efficiency of the neutron detector, is found to be a constant, which is about 17%, for the neutrons of kinetic energy above about 60 MeV.

References

[1] R. A. Cecil et al., Nucl. Instrum. Methods **161**, 439 (1979).

[2] V. McLane et al., **Neutron Cross Section, Curves, Volume 2**, Academic Press(1988).

[3] John. W. Watson, Private Communication.

Appendix A

The input file to the computer simulation code is different for bars of different heights. The Fig. A1 shows a typical file for a bar of 10 cm height. Note that all bars in the neutron detector have same length of 100 cm and same thickness of 10 cm. We need not change anything in the standard input file except the bar dimensisions and the desired input energy (Column for E1 in Fig.A1). The bar dimentions are 20.0 2.5 4.0 in inches just below the comment line $SCINTILLATOR\,BOUNDARIES\,(XB,\,YB,\,ZB\,all\,in\,INCHES),\,IGEO,\,IRANP\,(3F6.2,\,2I2)$ of the input file below where 20.0 (XB) is the half of the bar length and 2.5 (YB) is again half of the bar height while 4.0 (ZB) is bar thickness (no half here).

```
40 BY 4 BY 4 NE102 DETECTOR
SENSE SWITCH SETTINGS AND NUMBER OF EVENTS TO DUMP (6I1,I4):NSW,MDUMP
122222 0
BIAS(MEVEE),TIMING(NSEC)BIN WIDTH,POSITION(IN) FOR STUDY(3F8.3):TBIAS,DTIM,DPOS
0.2      0.1      0.2
TWO VALUES OF ONE-PE LEVEL(MEVEE) FOR RES. SMEARING (2F6.2):ELOPE(2),ELOPE(3)
0.002  0.02
SEED FOR RANDOM NUMBER GENERATOR (I5):KS1,KS2
2223   0
DENSITY (GM/CM**3) AND RATIO OF H TO C ATOMS (2F8.3):RHO, COMP
1.032   1.104
LIGHT OUTPUT COEF. FOR PROTONS (6F12.5): PA,PB,PC,PR,PS,PT
-8.0000     -.10000     .90000000   .95         0.0         0.0
LIGHT OUTPUT COEF. FOR ALPHAS (6F12.5): AH,AO,AP,AQ,AU
-5.90000    -.065       1.01        .41         0.0         0.0
SCINTILLATOR BOUNDARIES(XB,YB,ZB all in INCHES),IGEO,IRANP (3F6.2,2I2)
20.0   2.0   4.0   0 1
POSITIONS          DIRECTION COSINES    ENERGY  DELTA E  COUNTS BINWIDTH
-*-(XI(I),I=1,3)   (CI(I),I=1,3)         E1       DE     NEV     BINW
40" X 4" X 4" DEEP NE-102 DETECTOR
0.0  0.0  0.0   0.0    0.0    1.0    20.0     0.0  100000    .10
0.0  0.0  0.0   0.0    0.0    1.0    30.0     0.0  100000    .10
0.0  0.0  0.0   0.0    0.0    1.0    40.0     0.0  100000    .10
0.0  0.0  0.0   0.0    0.0    1.0    50.0     0.0  100000    .10
0.0  0.0  0.0   0.0    0.0    1.0    60.0     0.0  100000    .10
0.0  0.0  0.0   0.0    0.0    1.0    70.0     0.0  100000    .10
0.0  0.0  0.0   0.0    0.0    1.0    80.0     0.0  100000    .10
0.0  0.0  0.0   0.0    0.0    1.0    90.0     0.0  100000    .10
0.0  0.0  0.0   0.0    0.0    1.0    100.0    0.0  100000    .10
0.0  0.0  0.0   0.0    0.0    1.0    110.0    0.0  100000    .10
0.0  0.0  0.0   0.0    0.0    1.0    120.0    0.0  100000    .10
0.0  0.0  0.0   0.0    0.0    1.0    130.0    0.0  100000    .10
0.0  0.0  0.0   0.0    0.0    1.0    140.0    0.0  100000    .10
0.0  0.0  0.0   0.0    0.0    1.0    150.0    0.0  100000    .10
0.0  0.0  0.0   0.0    0.0    1.0    160.0    0.0  100000    .10
0.0  0.0  0.0   0.0    0.0    1.0    175.0    0.0  100000    .10
```

Fig. A1: Input file to the Kent State University computer simulaton code

Appendix B

Table 1 shows the data used in the plots of Fig.3. Since the third plane contains bars of mixed heights, we supply the height of 12.5 cm in the input file of the simulation code for a bar in that plane.

Kinetic Energy	**Efficiency (%) of a Neutron bar in**			
(MeV)	First Plane	Second Plane	Third Plane	Fourth Plane
20.0	4.948	7.636	8.154	0.078
30.0	7.039	8.225	8.5	5.355
40.0	8.093	9.509	9.804	5.972
50.0	9.567	10.924	11.44	7.899
60.0	10.324	11.459	11.64	8.62
70.0	10.147	11.024	11.283	8.958
80.0	10.049	10.667	10.827	8.982
90.0	9.754	10.337	10.505	9.072
100.0	9.555	10.007	10.175	8.893
110.0	9.649	10.172	10.223	9.095
120.0	9.342	9.654	9.759	8.663
130.0	9.134	9.547	9.709	8.674
140.0	9.104	9.439	9.567	8.57
150.0	9.0	9.448	9.552	8.732
160.0	8.87	9.355	9.451	8.47
175.0	9.033	9.451	9.51	8.754

Table 1: Efficiency of different neutron counters at different neutron kinetic energies. [Table for Fig. 3]

Appendix C

The removal cross section (i.e., non elastic cross section) in barn of various elements and materials are given in the following table. Here the non-elastic cross section for Pb, Fe and C are directly read from the reference [2] and that for air is obtained from the reference [3]. Removal cross section for plastic is calculated from the information of C and H assuming that the plastic is made up of C and H only in the H to C ratio 1.104. Note that the removal cross section of H is taken as the two thirds of its total cross section since its non-elastic cross section is not available in the reference [2] which is an exhaustive reference of all types of neutron cross sections reported to date.

Kinetic Energy	**Removal Cross section (barn)**					
(MeV)	Pb	Fe	C	H	Plastic	Air
20.0	2.6	1.25	0.50	0.33	0.41	0.201
30.0	2.5	1.00	0.42	0.20	0.305	0.249
40.0	2.4	0.95	0.36	0.15	0.25	0.232
50.0	2.3	0.9	0.32	0.11	0.21	0.197
60.0	2.2	0.8	0.26	0.09	0.171	0.160
70.0	2.0	0.78	0.22	0.07	0.142	0.137
80.0	1.9	0.76	0.21	0.06	0.13	0.114
90.0	1.85	0.74	0.22	0.05	0.131	0.091
100.0	1.8	0.73	0.23	0.047	0.135	0.077
110.0	1.75	0.71	0.23	0.043	0.133	0.066
120.0	1.7	0.70	0.24	0.04	0.135	0.056
130.0	1.65	0.68	0.23	0.039	0.13	0.050
140.0	1.6	0.66	0.22	0.037	0.124	0.048
150.0	1.55	0.65	0.21	0.033	0.117	0.048
160.0	1.52	0.65	0.20	0.031	0.116	0.048
175.0	1.5	0.60	0.19	0.030	0.116	0.048

Table 2: Removal cross section of Pb, Fe, C, H, plastic and air at various kinetic energy of neutron.

Appendix D

In this appendix we give all other data sets that we used in histograming all the remaining plots (after Fig. 3) in the main text. This appendix contains altogether five tables (Table 3 to Table 7). Table 3 shows the data of transmittance of various materials. Note that the following thicknesses of the materials that stay between the target (at the hall center of HallA) and the neutron detector: Air 600 cm, lead in the lead wall 5.08 cm, iron in the lead wall 4 cm, plastic in three planes in BigBite bars 3.55 cm, two overlaping veto bars 4 cm. Also note that any neutron counter in the neutron detector has thickness of 10 cm.

The nubmer density (n), length (L) and n∗L for various subtances are:
Lead: $n = 0.03300{*}10^{24}\ cm^{-3}$, $L = 5.08\ cm$, $nL = 0.16774{*}10^{24}\ cm^{-2}$
Iron: $n = 0.08460{*}10^{24}\ cm^{-3}$, $L = 4.00\ cm$, $nL = 0.33853{*}10^{24}\ cm^{-2}$
Plastic: $n = 0.99784{*}10^{23}\ cm^{-3}$, $L = 7.55\ cm$, $nL = 0.75336{*}10^{24}\ cm^{-2}$
Air: $n = 0.00270{*}10^{22}\ cm^{-3}$, $L = 600.0\ cm$, $nL = 0.01620{*}10^{24}\ cm^{-2}$

Kinetic Energy	**Transmittance**						
(MeV)	Pb	Fe	Air	Plastic−1	Plastic−2	Plastic−3	Plastic−4
20.0	0.65	0.655	0.997	0.73	0.49	0.32	0.22
30.0	0.66	0.713	0.996	0.795	0.59	0.43	0.32
40.0	0.67	0.725	0.996	0.83	0.65	0.50	0.39
50.0	0.68	0.737	0.997	0.85	0.69	0.56	0.46
60.0	0.69	0.763	0.997	0.88	0.74	0.62	0.53
70.0	0.715	0.77	0.998	0.90	0.78	0.68	0.59
80.0	0.727	0.77	0.998	0.91	0.80	0.70	0.61
90.0	0.73	0.78	0.999	0.91	0.80	0.70	0.61
100.0	0.74	0.78	0.999	0.90	0.79	0.69	0.60
110.0	0.746	0.786	0.999	0.90	0.79	0.69	0.61
120.0	0.75	0.79	0.999	0.90	0.79	0.69	0.60
130.0	0.76	0.79	0.999	0.91	0.80	0.70	0.61
140.0	0.765	0.80	0.999	0.91	0.80	0.71	0.63
150.0	0.77	0.80	0.999	0.92	0.81	0.72	0.65
160.0	0.775	0.80	0.999	0.92	0.82	0.73	0.65
175.0	0.78	0.816	0.999	0.92	0.82	0.73	0.65

Table 3. Transmittance of Pb, Fe, air, 7.55 cm thick plastic (Plastic−1), 17.55 cm thick plastic(Plastic−2) ,27.55 cm thick plastic (Plastic−3) and 37.55 cm thick plastic (Plastic−4) at various neutron kinetic energies.

Kinetic Energy (MeV)	**Factor**			
	Plane−1	Plane−2	Plane−3	Plane−4
20.0	1	0.67	0.44	0.30
30.0	1	0.74	0.54	0.40
40.0	1	0.78	0.60	0.47
50.0	1	0.81	0.66	0.54
60.0	1	0.84	0.70	0.60
70.0	1	0.87	0.76	0.66
80.0	1	0.88	0.77	0.67
90.0	1	0.88	0.77	0.67
100.0	1	0.88	0.77	0.67
110.0	1	0.88	0.77	0.67
120.0	1	0.88	0.77	0.67
130.0	1	0.88	0.77	0.67
140.0	1	0.88	0.78	0.69
150.0	1	0.88	0.78	0.71
160.0	1	0.89	0.79	0.71
175.0	1	0.89	0.79	0.71

Table 3A. The Factor is the number which is the ratio of transmittance of all plastic before the plane under consideration to the transmittance of all plastic before plane 1. Shown here is the Factor for various planes at various kinetic energy of neutrons.

Kinetic Energy (MeV)	**Transmittance of different Combination of materials**			
	Combination−1	Combination−2	Combination−3	Combination−4
20.0	0.31	0.21	0.134	0.092
30.0	0.37	0.27	0.198	0.147
40.0	0.40	0.31	0.24	0.187
50.0	0.42	0.34	0.277	0.228
60.0	0.46	0.385	0.320	0.276
70.0	0.49	0.426	0.370	0.320
80.0	0.50	0.444	0.390	0.340
90.0	0.51	0.452	0.396	0.345
100.0	0.515	0.453	0.395	0.344
110.0	0.52	0.46	0.40	0.356
120.0	0.53	0.465	0.410	0.353
130.0	0.54	0.478	0.420	0.364
140.0	0.555	0.487	0.430	0.384
150.0	0.56	0.497	0.440	0.40
160.0	0.57	0.51	0.45	0.40
175.0	0.58	0.52	0.45	0.41

Table 4: Transmittance of different combination of materials at various neutron kinetic energies. Combination−1 is Pb, Fe, Air and 7.55 cm thick plastic. Combination−2 is Pb, Fe, Air and 17.55 cm thick plastic. Combination−3 is Pb, Fe, Air and 27.55 cm thick plastic. Combination−4 is Pb, Fe, Air and 37.55 cm thick plastic.[Table for Fig. 4]

Kinetic Energy	**Transmittance with error of a Combination of materials**	
(MeV)	Combination−1	Statistical Error in Transmittance
20.0	0.31	0.053
30.0	0.37	0.054
40.0	0.40	0.055
50.0	0.42	0.054
60.0	0.46	0.055
70.0	0.49	0.054
80.0	0.50	0.053
90.0	0.51	0.052
100.0	0.515	0.052
110.0	0.52	0.051
120.0	0.53	0.050
130.0	0.54	0.050
140.0	0.555	0.050
150.0	0.56	0.049
160.0	0.57	0.049
175.0	0.58	0.045

Table 5: Transmittance with error bars of a combination of materials at various neutron kinetic energies. Combination−1 is Pb, Fe, Air and 7.55 cm thick plastic.[Table for Fig. 5]

Kinetic Energy (MeV)	**Detection Efficiency (%)**				
	Plane 1	Plane 2	Plane 3	Plane 4	Sum of all
20.0	1.534	1.603	1.092	0.007	4.236
30.0	2.604	2.22	1.683	0.787	7.294
40.0	3.237	2.947	2.353	1.116	9.653
50.0	4.018	3.714	3.169	1.801	12.702
60.0	4.749	4.411	3.725	2.379	15.264
70.0	4.972	4.685	4.174	2.866	16.697
80.0	5.024	4.736	4.222	3.054	17.036
90.0	4.974	4.672	4.16	3.129	16.935
100.0	4.921	4.533	4.019	3.059	16.532
110.0	5.017	4.679	4.089	3.238	17.023
120.0	4.951	4.489	4.001	3.058	16.499
130.0	4.932	4.563	4.078	3.157	16.73
140.0	5.052	4.596	4.114	3.291	17.053
150.0	5.04	4.695	4.203	3.492	17.433
160.0	5.056	4.771	4.253	3.39	17.38
175.0	5.239	4.914	4.374	3.589	18.116

Table 6: The detection efficiency of different planes at various kinetice energy of neutrons. The last column is the sum of the data of all previous four columns. Note that the detection efficiency is the product of efficiency and transmittance as defined in the text. [Table for Fig. 6]

Kinetic Energy (MeV)	**Sum of (Efficiency $*$ Factor) of four planes** %	**Transmittance of all materials before plane 1** %	**Product of both** %
20.0	13.683	31	4.24
30.0	19.86	37	7.35
40.0	24.2	40	9.68
50.0	30.23	42	12.7
60.0	33.26	46	15.3
70.0	34.23	49	16.77
80.0	33.8	50	16.9
90.0	33.02	51	16.84
100.0	32.16	51.5	16.56
110.0	32.56	52	16.93
120.0	31.15	53	16.51
130.0	30.82	54	16.64
140.0	30.78	55.5	17.08
150.0	30.96	56	17.34
160.0	30.68	57	17.49
175.0	31.17	58	18.08

Table 7: The second column is the sum of (efficiency $*$ factor) of all the four planes calculated by different approach (see the text about Fig. 7). The third column is the transmittance of all materials present before the first plane. The last column is the product of second and third column′s data. [Table for Fig. 7]